

# Skutterudite vs. $\text{ReO}_3$ structures for $\text{MX}_3$ solids: electronic requirements ‡

Miquel Lluell, Santiago Alvarez and Pere Alemany \*†

Departament de Química Física and Departament de Química Inorgànica,  
 Universitat de Barcelona, Diagonal 647, 08028 Barcelona, Spain

Electronic band-structure calculations on  $\text{ReO}_3$  and  $\text{CoP}_3$  have been performed to analyse the different structural preferences found for these two compounds. The electronic origin of these differences is associated with the formation of the characteristic non-metal four-membered rings of the skutterudite structure, which is energetically unfavorable for compounds with small, strongly electronegative anions. The combination of two factors has been identified to be responsible for the structural differences between these compounds. The first is the electronegativity difference between the two types of atoms that form the solid: for strongly electronegative non-metal atoms like O or F the  $\text{ReO}_3$ -type structure is expected to be the most stable, while for the combination of less electronegative atoms like the pnictides with late transition metals the skutterudite structure is preferred. The second factor is the relative size of the constituting atoms: small atoms like F and O favor the  $\text{ReO}_3$  structure, while larger atoms like P and As stabilize the skutterudite one.

Transition-metal pnictides (N, P, As, Sb or Bi) form a vast family of compounds that exhibit a very rich structural variation, crystallizing in a large number of different structural types. This family can be roughly divided into two distinct groups based on the stoichiometry of the compounds, comprising metal-rich phases on the one hand and pnictide-rich ones on the other. The structures of the compounds belonging to the first group are characterized by extensive metal-metal bonding, while pnictide atoms appear as single anions or discrete diatomic units. The large number of structures found for the second group can be attributed to the high versatility of pnictides in forming complex anionic structures which comprise clusters, chains, sheets or three-dimensional arrays of covalently bound pnictide atoms. The metal atoms in these compounds occupy the holes left by the anionic sublattice. The structural richness for these compounds is translated into their physical properties. Among transition-metal pnictides one can find metals, semiconductors and superconductors as well as different types of magnetic behavior.

Pnictides of Group 9 and 10 transition metals with  $\text{MX}_3$  stoichiometry adopt the skutterudite structure,<sup>1</sup> which has isolated, almost square  $\text{X}_4$  rings as its most prominent feature. Although the electronic structure of these compounds and its relation to their electrical properties has been addressed using different theoretical approaches,<sup>2-4</sup> a deep understanding of the bonding in skutterudite phases is still lacking. In this contribution we report semiempirical band-structure calculations of the extended-Hückel type used to explore the nature of the chemical bonding in these compounds. Special attention will be devoted to the electronic requirements needed to form the characteristic  $\text{X}_4$  rings present in the skutterudite structure as well as its relation to the more symmetrical  $\text{ReO}_3$ -type crystal structure.

## Results and Discussions

### The $\text{ReO}_3$ and skutterudite crystal structures

From a topological standpoint the  $\text{ReO}_3$  structure (space group  $\text{Pm}\bar{3}\text{m}$ , no. 221)<sup>5,6</sup> is the simplest framework structure for a

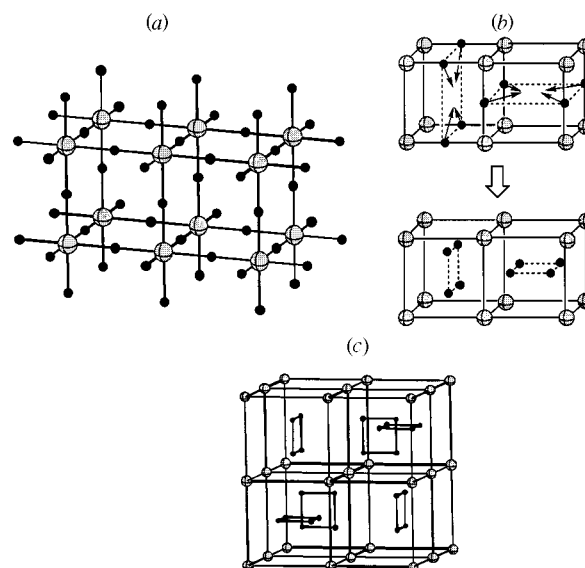


**Fig. 1** (a) The  $\text{ReO}_3$  crystal structure. Black and white circles represent oxygen and rhenium atoms, respectively. (b) To derive the skutterudite structure from the  $\text{ReO}_3$  structure one can displace the non-metal atoms (black spheres) located on the four parallel edges of a metal cube to its center. (c) The skutterudite ( $\text{CoAs}_3$ ) crystal structure. Black and white circles represent non-metal and metal atoms, respectively

$\text{MX}_3$  compound built of octahedral  $\text{MX}_6$  groups. Each  $\text{MX}_6$  octahedron shares a common vertex with six neighboring octahedra, giving a simple cubic array of M atoms [Fig. 1(a)]. In this simple arrangement all  $\text{MX}_6$  octahedra are oriented in the same direction, with all  $\text{M-X-M}$  angles equal to  $180^\circ$ .

Occupation of the body center of a simple cubic lattice of metal atoms with large ions gives the well known perovskite structure for  $\text{MBX}_3$  compounds,<sup>1</sup> in which B and X atoms together form a cubic close packed assembly.

The skutterudite structure (space group  $\text{Im}\bar{3}$ , no. 204)<sup>7-11</sup> is related in a rather simple way to the more symmetric  $\text{ReO}_3$  structure. The characteristic  $\text{X}_4$  rings present in skutterudites can be obtained by displacing four of the non-metal atoms located on parallel edges of a metal cube to its center, as shown in Fig. 1(b) for two adjacent metal cubes. Since each of these

† E-Mail: pere@linus.qui.ub.es

‡ Non-SI unit employed: eV  $\approx 1.60 \times 10^{-19}$  J.

cubes has X atoms on its twelve edges, the displacement toward the interior of a cube also affects eight neighboring cubes. The new unit cell is thus eight times larger than the original  $\text{ReO}_3$  unit cell. From the directions in which the various sets of X atoms are moved it follows that one quarter of the metal cubes will not contain an  $\text{X}_4$  unit in its interior [Fig. 1(c)].

In the resulting skutterudite structure each M atom is still in an octahedral environment with each  $\text{MX}_6$  octahedron sharing its six vertices with six neighboring octahedra as in  $\text{ReO}_3$ . The main differences between the two structures are that in the case of skutterudites the  $\text{MX}_6$  octahedra are slightly distorted ( $D_{3d}$  symmetry), with their relative orientations in the three-dimensional array tilted (M–X–M angles smaller than  $180^\circ$ ). The  $\text{X}_4$  rings are not square, the lengths of the sides of the rectangles being slightly different (2.46 and 2.57 Å in  $\text{CoAs}_3$ ).<sup>9</sup>

We have noted above that the perovskite structure can be derived from the  $\text{ReO}_3$ -type structure by filling the large cuboctahedral holes, of which there is one per  $\text{ReO}_6$  octahedron. In the skutterudite structure three out of every four holes are occupied by the  $\text{X}_4$  rings. Filling of the remaining holes by a rare-earth metal R gives the ternary  $\text{RM}_4\text{X}_{12}$  compounds<sup>12–17</sup> which are often called filled skutterudites.

In the electronic structure calculations reported below we will in some cases use idealized skutterudite structures in which one has either square  $\text{X}_4$  rings or regular  $\text{MX}_6$  octahedra. The relation between these idealized structures and the real skutterudite structure will thus be analysed first. The geometry of the skutterudite structure is totally determined by three parameters:<sup>8–11</sup> the cell edge  $a$  and two parameters ( $y$  and  $z$ ) that define the crystallographic coordinates of the X atoms in the 24g positions of the space group. For the  $\text{ReO}_3$  structure these two last parameters are required by symmetry to adopt a value of  $y = z = 0.25$ . In the idealized skutterudite with regular  $\text{MX}_6$  octahedra  $y$  and  $z$  are related through equation (1), while in

$$8y(2z - 1) = 8z - 3 \quad (1)$$

the case of square  $\text{X}_4$  rings these two parameters must obey equation (2).

$$2(y + z) = 1 \quad (2)$$

The  $\text{ReO}_3$ -type structure corresponds to the case in which both equations are satisfied simultaneously. If one plots the  $y$  and  $z$  values for the different experimentally determined skutterudite structures (Fig. 2) it is clear that they are all much closer to the case with square  $\text{X}_4$  rings [equation (2)] than to that with regular  $\text{MX}_6$  octahedra [equation (1)].

A single parameter,  $\xi$ , will be used throughout this paper to indicate the extent to which a given skutterudite differs from its parent  $\text{ReO}_3$ -type structure. For a given  $\text{MX}_3$  compound  $\xi$  is defined as the ratio between the actual cell edge  $a$  of the skutterudite unit cell and the unit cell edge  $a^\circ$  of an hypothetical  $\text{ReO}_3$ -type structure with the same M–X bond length as in the real  $\text{MX}_3$  skutterudite. Since the rotation and deformation of the  $\text{MX}_6$  octahedra that is necessary to generate the skutterudite structure from its parent  $\text{ReO}_3$ -type structure results in a shortening of the unit-cell edge,  $\xi$  will always take values between 0 and 1. Compounds which crystallize in the  $\text{ReO}_3$ -type structure have  $\xi = 1$  while those with the skutterudite structure adopt values of  $\xi$  in the range 0.85–0.90 (see Table 1).

The skutterudite structure is found only for Group 9 and 10 transition-metal pnictides, although not all possible metal/non-metal combinations are found. No  $\text{MX}_3$  nitrides are known, probably due to the small size of the nitrogen atoms that would give a skutterudite structure with too short M–M distances to be stable. On the other hand, bismuth compounds with  $\text{MBi}_3$  composition are known,<sup>32,33</sup> but they adopt other structures. In this case the large size of the bismuth atoms would give skutterudites with too large M–M distances to be stable.

**Table 1** Values of the structural parameter  $\xi$  (see text for definition) for different compounds which crystallize in the  $\text{ReO}_3$  or skutterudite-type structures<sup>31</sup>

Compound	$\xi$	Ref.	Compound	$\xi$	Ref.
$\text{CoP}_3$	0.87	8	$\text{RhAs}_3$	0.87	9
$\text{NiP}_3$	0.86	8	$\text{IrAs}_3$	0.87	9
$\text{RhP}_3$	0.85	8	$\text{CoSb}_3$	0.90	9
$\text{IrP}_3$	0.85	8	$\text{RhSb}_3$	0.88	9
$\text{CoAs}_3$	0.88	9	$\text{IrSb}_3$	0.88	9
$\text{Fe}_{0.5}\text{Ni}_{0.5}\text{Sb}_3$	0.90	9	$\text{Co}_2\text{Ge}_3\text{S}_3$	0.88	18
$\text{RM}_4\text{X}_{12}$	0.87–0.89	12–17	$\text{MF}_3$	1.00	19–21
$\text{ReO}_3$	1.00	5, 6	$\text{A}_x\text{MO}_3$	>0.96	23–30
$\text{ReO}_3^*$	0.99	22			

\* High pressure form.

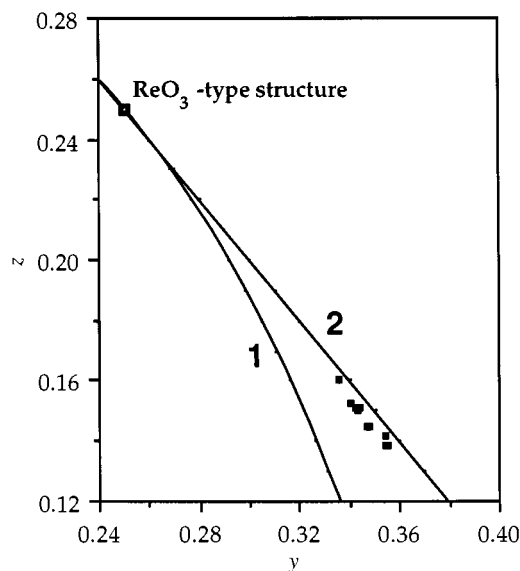


**Fig. 2** Relation between  $y$  and  $z$  for different symmetry conditions:  $\text{ReO}_3$ -type structure ( $y = z = 0.25$ ), idealized skutterudite structures with regular  $\text{MX}_6$  octahedra (curve 1) or with square  $\text{X}_4$  rings (curve 2). Single points correspond to experimental values for different skutterudites

Other compounds that are known to crystallize in the skutterudite structure are the ternary  $\text{M}_2\text{X}_3\text{Y}_3$ <sup>18,34</sup> and  $\text{M}_x\text{M}'_{1-x}\text{X}_3$ <sup>9,35–38</sup>. The full crystal structure has only been examined for  $\text{Co}_2\text{Ge}_3\text{S}_3$ <sup>18</sup> and for  $\text{Fe}_{0.5}\text{Ni}_{0.5}\text{Sb}_3$ .<sup>9</sup> For these compounds,  $\xi$  is found to take a value of 0.88 and 0.90, respectively, in the same range as for the skutterudite-type pnictides.

The introduction of rare-earth-metal cations into the skutterudite structure to give the filled skutterudites does not alter the basic arrangement of atoms in the  $\text{MX}_3$  net as can be seen by comparing the values of  $\xi$  between 0.87 and 0.89 found for these compounds<sup>12–17</sup> with those for the parent skutterudite-type binary phases.

On the other hand, the more symmetrical  $\text{ReO}_3$ -type structure is only found for a small number of compounds:  $\text{ReO}_3$ <sup>5,6</sup> and some transition-metal fluorides ( $\text{MF}_3$  with  $\text{M} = \text{Mo}, \text{Nb}$  or  $\text{Ta}$ ).<sup>19–21</sup> Interestingly, a skutterudite-type distortion is found at high pressure for  $\text{ReO}_3$ .<sup>22</sup> The displacement of atoms is nevertheless small and the  $\text{O}\cdots\text{O}$  distances still remain long enough so that they cannot be considered as actual bonds. The value of 0.99 found for  $\xi$  indicates that it is much closer to the original  $\text{ReO}_3$ -type structure than to the skutterudite one. Another way to force a skutterudite distortion in  $\text{ReO}_3$  is by introducing some extra cations in it. Compounds  $\text{A}_x\text{MO}_3$ , where A is either H, Li or Na and M is Nb, Mo, Ta, W or Re are known.<sup>23–30</sup> The inclusion of A atoms induces a compression of the original  $\text{ReO}_3$  framework by tilting the  $\text{ReO}_6$  octahedra rather than compressing them. The Re–O distances in  $\text{D}_{1,36}\text{ReO}_3$ <sup>25</sup> and  $\text{Li}_{0.2}\text{ReO}_3$ <sup>30</sup> are at most 0.04 Å larger than in  $\text{ReO}_3$ . These phases have  $\xi$  values around 0.96 indicating that despite the

noticeable compression they still have structures closer to  $\text{ReO}_3$  than those of the skutterudite-type transition-metal pnictides.

All these data suggest that the more symmetric  $\text{ReO}_3$ -type structure is only favored over the 'distorted' skutterudite one when some electronic and size requirements are fulfilled. The following two criteria seem to be necessary for a  $\text{ReO}_3$ -type structure to be stable: (1) strongly electronegative X atoms; (2) small, first-row X atoms.

In the following section we will analyse the electronic structure in both  $\text{ReO}_3$ - and skutterudite-type compounds, in a search for the origin of the electronic requirements that underlie the structural choice in this type of  $\text{MX}_3$  crystals. An additional complication that has to be kept in mind is that a third variable, the number of valence electrons per formula unit, has to be included in the analysis since the compounds we want to compare are not isoelectronic. Group 9 transition-metal pnictides have a total of 24 valence electrons,  $\text{ReO}_3$  and  $\text{NiP}_3$  have 25, and the  $\text{MF}_3$  fluorides 26 or 27, depending on the metal.

### Electronic structure of $\text{ReO}_3$ and $\text{CoP}_3$

The electronic structure of  $\text{ReO}_3$  and of skutterudite-type pnictides has been previously analysed by various authors using different theoretical approaches. Corà *et al.*<sup>39</sup> presented recently the results of an electronic structure study for  $\text{WO}_3$ ,  $\text{ReO}_3$  and  $\text{NaWO}_3$  using both the full potential linear muffin-tin orbital (FP-LMTO) and the periodic Hartree-Fock method. Although these authors did not study the possibility of a skutterudite-type structure for these oxides, their calculations suggest that the cubic structure which is experimentally found for  $\text{ReO}_3$  is remarkably stable and rigid, a fact which they associate with the presence of antibonding conduction electrons.

The structural choice in skutterudite-type pnictides has, to our knowledge, never been studied before. Some work has been devoted to the band structure and bonding in some compounds like  $\text{CoSb}_3$ ,<sup>3</sup>  $\text{CoP}_3$ ,<sup>4</sup> and  $\text{NiP}_3$ ,<sup>4</sup> using first principles, DFT-based methods. In these works the experimental structure is assumed for each compound and the stability of alternatives is not considered. In recent times the electronic structure of skutterudites and their lattice dynamics have been also investigated in connection with the search for new improved thermoelectric materials.<sup>40,41</sup>

To analyse the electronic factors that dictate the structural choice in  $\text{MX}_3$  compounds we have performed extended-Hückel tight-binding band-structure calculations<sup>42-44</sup> for  $\text{ReO}_3$  and  $\text{CoP}_3$ , using two different structures in each case: the experimental one and the hypothetical alternative. Structural details for these idealized phases and information related to the computational procedure can be found in the Appendix.

Since its original formulation the extended-Hückel method has been successfully applied to the study of bonding in a large number of compounds including molecules, surfaces and solids.<sup>45,46</sup> Although based on rather crude approximations the method is especially well suited for complex systems, such as the skutterudite-type structures. This is due mainly to its simplicity, both computationally and conceptually. Extended-Hückel calculations should permit us to extract a qualitative picture of the different bonding situations and their structural implications for the compounds under study. It is clear that the relative energies obtained for different structures of a same compound can in no way be taken in a quantitative fashion. The calculated trends should nevertheless be essentially correct for moderate distortions around the experimental geometry in cases like ours, where the nearest-neighbor distances (M-X) remain unchanged.

Fig. 3 shows the density of states (DOS) curve calculated for  $\text{ReO}_3$  using its experimentally determined crystal structure. The three well separated regions that can be identified in this curve correspond mainly to the oxygen 2p orbitals (peak between -17 and -14 eV) and the rhenium 5d orbitals that show the

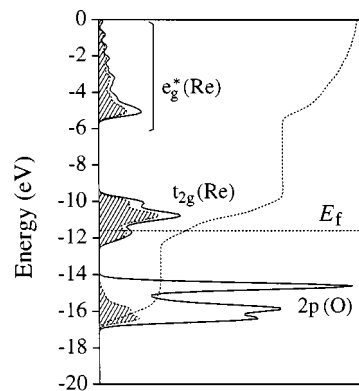


**Fig. 3** The DOS curve for  $\text{ReO}_3$  at its experimental crystal structure. The shaded area and the dashed curve correspond to the contribution of the d orbitals of rhenium and to the integrated DOS for this contribution, respectively

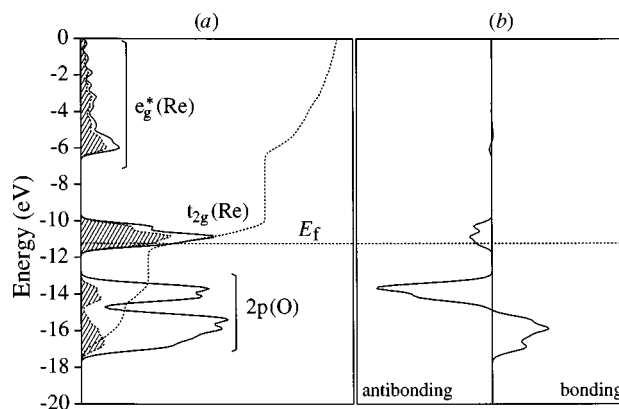


**Fig. 4** The DOS (a) and O...O COOP (b) curves for  $\text{ReO}_3$  with the skutterudite-type crystal structure. In (a) the shaded area and the dashed curve correspond to the contribution of the d orbitals of rhenium and to the integrated DOS for this contribution, respectively

typical  $t_{2g}$  (peak between -12 and -10 eV) below  $e_g$  (peak between -5 and 0 eV) splitting of the d orbitals in an octahedral environment. The Fermi level ( $E_f$ ) corresponding to a metal  $d^1$  configuration is located at the bottom of the  $t_{2g}$  band.

When  $\text{ReO}_3$  is forced to adopt a skutterudite-type structure major changes in the DOS [Fig. 4(a)] are found only in the O 2p region, while the Re 5d bands remain located approximately in the same energy ranges as in the DOS curve calculated for the experimental structure. The O 2p band is now split into two peaks, that spread between -17 and -14 eV. An analysis of the bonding characteristic of these states using the O...O COOP (crystal orbital overlap population) curve in Fig. 4(b) indicates that the low-lying peak is O...O bonding for the  $\text{O}_4$  rings present in the structure, while the higher peak is antibonding. The integrated COOP curve has a negative value at the Fermi level, indicating a net repulsive O...O interaction for this structure. Our calculations suggest that the formation of electron-rich  $\text{O}_4^{8-}$  rings in this highly ionic structure should be strongly disfavored from an energy point of view. It is also clear that removing one valence electron per formula unit to achieve a system isoelectronic with  $\text{CoP}_3$  will not result in an important stabilization of the skutterudite-type structure relative to the  $\text{ReO}_3$  one since deep-lying O...O antibonding levels would still remain filled in this case.

A plot of the one-electron energy for  $\text{ReO}_3$  as a function of  $\xi$  [Fig. 5(a)] shows clearly that the  $\text{ReO}_3$ -type structure is more stable than the skutterudite one. As can be appreciated, the path chosen to produce the skutterudite-type structure (regular

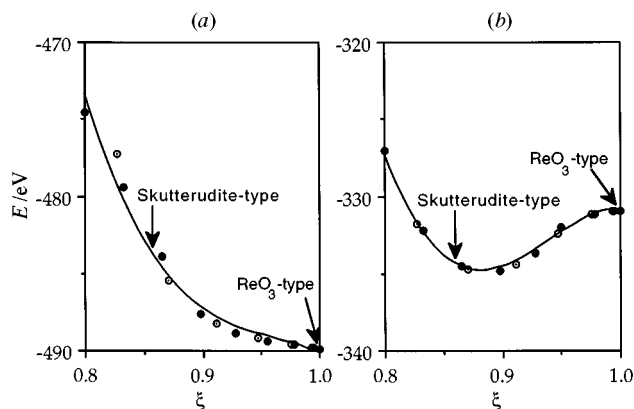


Fig. 5 Dependence on the structural parameter  $\xi$  of the one-electron energy for  $\text{ReO}_3$  (a) and  $\text{CoP}_3$  (b)

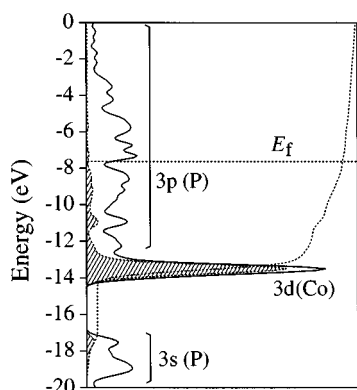


Fig. 6 The DOS curves for  $\text{CoP}_3$  with  $\text{ReO}_3$ -type crystal structure. The shaded area and the dashed curve correspond to the contribution of the d orbitals of cobalt and to the integrated DOS for this contribution, respectively

octahedra or square  $\text{O}_4$  rings) results only in minor energy differences, indicating that any reasonable skutterudite structure with  $y$  and  $z$  values between these two limiting cases will be unstable if compared with the experimental crystal structure of  $\text{ReO}_3$ . The steep energy increment calculated for structures with decreasing  $\xi$  values is in good agreement with the small departures from the  $\text{ReO}_3$ -type structure observed for this compound under pressure or for its  $\text{A}_x\text{ReO}_3$  derivatives.

Let us now move to  $\text{CoP}_3$ . The DOS curve for this compound adopting an hypothetical  $\text{ReO}_3$ -type structure is presented in Fig. 6. This plot is totally different from that in Fig. 3. The levels under  $-17$  eV correspond mainly to phosphorus 3s orbitals. The sharp peak centered around  $-13.5$  eV is built up of cobalt 3d orbitals. A more careful analysis shows that the lowest part of this peak is formed by Co–P combinations of  $e_g$  symmetry while the upper part corresponds mainly to Co–P non-bonding levels of  $t_{2g}$  symmetry. This ‘inverse’ splitting situation for the 3d levels of cobalt, which arises from the strong covalent nature of Co–P bonds in this crystal, has been previously described in detail and is found to be quite common for late transition-metal pnictides.<sup>4,47</sup> The region of the DOS lying directly over this sharp metal peak is occupied by a wide band formed mainly by the 3p orbitals of the phosphorus atoms. The Fermi level for this hypothetical compound is found in a small pseudo-gap located approximately at the middle of this wide band.

What happens if we repeat the calculations using the experimental skutterudite-type structure for  $\text{CoP}_3$ ? The DOS curve presented in Fig. 7(a) shows a splitting of the low lying P 3s and the wide P 3p bands. A gap is opened around the Fermi level, in good agreement with the semiconducting behavior that has been experimentally determined for  $\text{CoP}_3$ . The metal 3d band is

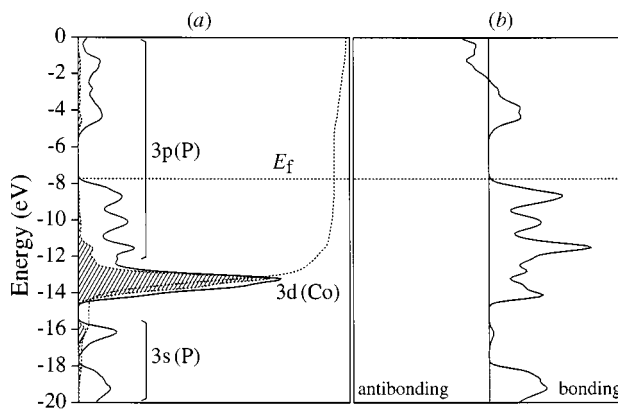
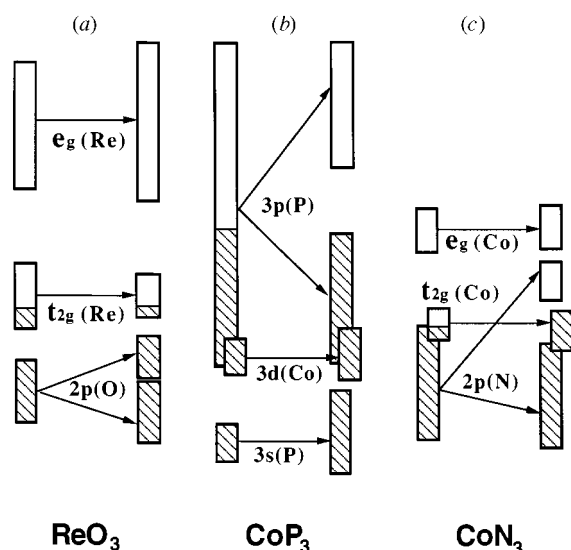


Fig. 7 The DOS (a) and P...P COOP (b) curves for  $\text{CoP}_3$  with the experimental skutterudite-type structure. In (a) the shaded area and the dashed curve correspond to the contribution of the d orbitals of cobalt and to the integrated DOS for this contribution, respectively

located approximately at the same energy as in the previous case, showing only a slight broadening with the structural change. The small spatial extent of the d orbitals of the transition metals is responsible for the small changes observed for these levels in the DOS when changing the structure. Their situation in the DOS curve is mainly dictated by their first coordination sphere, which is practically the same in both structures. From the COOP curve presented in Fig. 7(b) we can easily convince ourselves that the formation of  $\text{P}_4$  rings in  $\text{CoP}_3$  will be an energetically favorable process since all P...P antibonding states are pushed up too high in energy to be occupied by electrons. The bottom of the conduction band is built mainly from P...P slightly bonding or non-bonding states, indicating that a moderate increase in the valence electron number up to 25 or 26 electrons per formula unit will not result in an important destabilization of the  $\text{P}_4$  rings, a prediction that is confirmed by the existence of the 25-electron compound  $\text{NiP}_3$  in which the P...P distances are very similar to those found in  $\text{CoP}_3$ .

A plot of the one-electron energy for  $\text{CoP}_3$  as a function of  $\xi$  [Fig. 5(b)] presents a minimum in the region of  $\xi$  values found for the known skutterudite-type structures, indicating that the ring formation is favorable in this case. As was found for  $\text{ReO}_3$ , the path followed in the distortion of the symmetrical  $\text{ReO}_3$ -type structure results only in minor energy differences, indicating that for  $\text{CoP}_3$  the skutterudite-type structure with  $\xi$  around the experimental value (0.87) will be more stable than the symmetric  $\text{ReO}_3$ -type structure.

Our calculations on  $\text{ReO}_3$  and  $\text{CoP}_3$  show that, as experimentally found, the structural preferences for these two compounds are completely different. The origin of this difference can be found in the  $\text{X}_4$  ring-formation process. A general description of both situations is given schematically in Fig. 8. For  $\text{ReO}_3$ -type structures with strongly electronegative X atoms like O or F, the valence p orbitals form a low-lying, narrow band which is totally occupied by electrons. In these cases the metal d bands lie much higher in energy, well separated from this band. Bonding in these compounds is best described as ionic, with almost atomic-like orbitals on both types of atoms. When pushing the X atoms together to form the  $\text{X}_4$  rings, orbital interactions between the valence p orbitals on these atoms become more and more important. The formation of X–X bonding and antibonding orbitals (of both  $\sigma$  and  $\pi$  types relative to the ring plane) leads to the splitting of the X p band described above. Since these X p levels lie well under the partially filled metal d orbitals, the formation of  $\text{X}_4$  rings with reasonable X–X distances is not able to push the X–X antibonding combinations over the Fermi level, resulting in an energetically unfavorable process that can be described either as a closed-shell repulsion between the X atoms or coulombic repulsion between the  $\text{X}^{2-}$  anions in a perfectly ionic solid.



**Fig. 8** Schematic representation of the changes in the band structures of (a)  $\text{ReO}_3$ , (b)  $\text{CoP}_3$  and (c)  $\text{CoN}_3$ , when distorting the  $\text{ReO}_3$ -type structure (a) to a skutterudite-type one (c)

The situation is totally different in solids like  $\text{CoP}_3$ , where the electronegativity difference between the metal and the non-metal atoms is not very large. The bonding in the hypothetical  $\text{ReO}_3$ -type structure is better described as covalent. The total filling of the d band for the metal, together with the almost neutral charges calculated for the X atoms, agree well with this description. Strong interaction between metal- and X-centered orbitals gives a broad X p band, with the Fermi level located approximately at its center. Formation of  $\text{X}_4$  rings is energetically favored in this case since the X–X antibonding levels can be pushed over the Fermi level, while the total energy is lowered by the stabilization provided by the newly formed X–X bonds.

At a first sight it can be argued that, in the case of  $\text{ReO}_3$ , forming a ring with sufficiently short  $\text{O}\cdots\text{O}$  distances should be able to push the  $\text{O}\cdots\text{O}$  antibonding levels over the Fermi level, achieving an electronic structure similar to that found for  $\text{CoP}_3$  with the skutterudite structure. This situation is indeed reached in our calculations for reasonable  $\text{O}\cdots\text{O}$  distances ( $\approx 1.5 \text{ \AA}$ ) corresponding to values of  $\zeta$  around 0.8. A look at the energy for the hypothetical structure [Fig. 5(a)] shows that it is unstable relative to the experimentally found  $\text{ReO}_3$ -type structure. The reason is that the destabilization of the  $\text{O}\cdots\text{O}$  antibonding levels over the Fermi energy is associated with an electron transfer to the partially filled  $t_{2g}$  band, which is relatively high in energy when compared to the oxygen 2p band in the original  $\text{ReO}_3$  structure. The energy gain associated with the lowering of bonding  $\text{O}\cdots\text{O}$  levels is compensated by this charge transfer, resulting in a global destabilization. This transfer is not possible in  $\text{CoP}_3$  since the small electronegativity difference between Co and P leads to an ‘inverse’ splitting situation which results in an extensive filling of the metal levels. The distortion to the skutterudite structure raises only empty  $\text{P}\cdots\text{P}$  antibonding levels in this case. Stabilization of the skutterudite structure is obtained from the associated lowering of their filled bonding counterparts.

Our analysis identifies the electronegativity differences between M and X as an important parameter in determining the structural choice of  $\text{ReO}_3$  and the skutterudite-type transition-metal pnictides. Is there any effect of the size of the X atoms in the structural choice in  $\text{MX}_3$  solids? The size of X atoms is important in the determination of the width of bands that are involved in the ring-formation process: small atoms like O give rise to narrow bands, while larger atoms, like P, give rise to broader bands. The influence of anion size can easily be understood when examining the hypothetical  $\text{CoN}_3$  compound. The schematic band structure diagram in Fig. 8(c) indicates that

**Table 2** Atomic parameters used for the extended-Hückel calculations on  $\text{ReO}_3$  and  $\text{CoP}_3$

Atom	Ref.	Orbital	$H_{ii}/\text{eV}$	$\zeta_{ii}$
Re	49	6s	−9.36	2.40
		6p	−5.96	2.37
		5d <sup>a</sup>	−12.66	5.34
O	42	2s	−32.30	2.28
		2p	−14.80	2.28
Co	4	4s	−9.21	2.00
		4p	−5.29	2.00
		3d <sup>b</sup>	−13.18	5.55
P	4	3s	−18.40	1.81
		3p	−9.80	1.45

<sup>a</sup>  $c_1 = 0.6662$ ,  $\zeta_{12} = 2.28$ ,  $c_2 = 0.5910$ . <sup>b</sup>  $c_1 = 0.5680$ ,  $\zeta_{12} = 2.10$ ,  $c_2 = 0.6060$ .

the N 2p band for the  $\text{ReO}_3$ -type structure is much narrower than the corresponding P 3p band in  $\text{CoP}_3$ . Owing to the higher electronegativity of nitrogen, the band is also displaced to lower energies. The net effect of these two factors is a much lower filling of the metal d levels for  $\text{CoN}_3$  ( $\approx 20\%$ ) than for  $\text{CoP}_3$  ( $\approx 90\%$ ). When distorting the crystal to achieve a skutterudite-type structure, the  $\text{N}\cdots\text{N}$  antibonding levels are destabilized and pushed over the Fermi energy, while the electrons contained in them are being transferred to the metal d orbitals. The net effect is, as discussed above, a destabilization. Should this compound be synthesized, our calculations indicate that the  $\text{ReO}_3$ -type structure would be preferred over the skutterudite one.

## Conclusion

Electronic structure calculations on  $\text{ReO}_3$  and  $\text{CoP}_3$  show that, as found experimentally, these two compounds have completely different structural preferences. The origin of these can be associated with two main factors, the first and most important being the electronegativity difference between the types of atoms that form the solid. For strongly electronegative non-metal atoms like O or F the  $\text{ReO}_3$ -type structure is expected to be the most stable one while for the combination of less electronegative atoms like the pnictides with late transition metals the skutterudite structure is favored. The second factor affecting the structural choice is the relative size of the constituting atoms: small atoms like F and O favor the  $\text{ReO}_3$ -type structure, while larger atoms like P and As stabilize the skutterudite-type one. The electronic origin of these differences can be assigned to the formation of non-metal four-membered rings in the skutterudite structure which is found to be energetically unfavorable for small, strongly electronegative atoms.

## Appendix

All the band-structure calculations presented in this work have been made by using the extended-Hückel tight-binding method.<sup>42–44</sup> The off-diagonal elements of the Hamiltonian matrix have been evaluated using the modified Wolfsberg–Helmholz formula.<sup>48</sup> The atomic parameters used in these calculations are shown in Table 2. Parameters for P and Co have been taken from recent work on the electronic structure of skutterudite-type phosphides,<sup>4</sup> while those for Re and O were those proposed by Alvarez.<sup>50</sup> Numerical integrations over the irreducible wedge of the Brillouin zone have been performed using a 64 k-point mesh obtained by the geometrical method of Ramirez and Böhm.<sup>51</sup>

In the calculations for idealized phases for  $\text{CoP}_3$  and  $\text{ReO}_3$ , the values for  $y$  and  $z$  parameters were taken as equal to their experimental value in  $\text{CoP}_3$  for the skutterudite-type idealized structure of  $\text{ReO}_3$ , and equal to 0.25 for the  $\text{ReO}_3$ -type idealized structure of  $\text{CoP}_3$ . In the calculations for Fig. 5 these para-

meters obey either the regular  $\text{MX}_6$  octahedra relation or the square  $\text{X}_4$  rings one. The cell edge  $a$  was taken in such that the M–X distance equals the experimental one in each case.

## Acknowledgements

M. L. thanks Comissió Interdepartamental per la Recerca i Innovació Tecnològica (Generalitat de Catalunya) for a doctoral grant. The authors are grateful to E. Ruiz and E. Canadell for helpful comments on this work. Financial support was provided by the Direcció General de Enseñanza Superior through grant PB95-0848-C02-01 and CIRIT through grant 1995-SGR-00421. Computing resources at the Centre de Supercomputació de Catalunya (CESCA) were allocated in part by Fundació Catalana per a la Recerca (FCR) and Universitat de Barcelona.

## References

- 1 P. Villars and L. D. Calvert, *Pearson's Handbook of Crystallographic Data for Intermetallic Phases*, American Society for Metals, Metals Park, Ohio, 1986.
- 2 D. Jung, M.-H. Whangbo and S. Alvarez, *Inorg. Chem.*, 1990, **29**, 2252.
- 3 D. J. Singh and W. E. Pickett, *Phys. Rev. B*, 1994, **50**, 11 235.
- 4 M. Llunell, P. Alemany, S. Alvarez, V. P. Zhukov and A. Vernes, *Phys. Rev. B*, 1996, **53**, 10 605.
- 5 K. Meisel, *Z. Anorg. Allg. Chem.*, 1932, **207**, 121.
- 6 T.-S. Chang and P. Trucano, *J. Appl. Crystallogr.*, 1978, **11**, 286.
- 7 I. Oftedal, *Z. Kristallogr.*, 1928, **A66**, 517.
- 8 S. Rundqvist and N.-O. Ersson, *Ark. Kemi*, 1968, **30**, 103.
- 9 A. Kjekshus and T. Rakke, *Acta Chem. Scand., Ser. A*, 1974, **28**, 99.
- 10 N. Mandel and J. Donohue, *Acta Crystallogr., Sect. B*, 1971, **27**, 2288.
- 11 R. T. M. Dobbe, W. J. Lustenhouwer, M. A. Zakrzewski, K. Goubitz, J. Fraanje and H. Schenk, *Can. Mineral.*, 1994, **32**, 179.
- 12 W. Jeitschko and D. J. Braun, *Acta Crystallogr., Sect. B*, 1977, **33**, 3401.
- 13 D. J. Braun and W. Jeitschko, *J. Solid State Chem.*, 1980, **32**, 357.
- 14 D. J. Braun and W. Jeitschko, *J. Less-Common Met.*, 1980, **72**, 147.
- 15 D. J. Braun and W. Jeitschko, *J. Less-Common Met.*, 1980, **76**, 33.
- 16 N. T. Stetson, S. M. Kauzlarich and H. Hope, *J. Solid State Chem.*, 1991, **91**, 140.
- 17 C. B. H. Evers, L. Boonk and W. Jeitschko, *Z. Anorg. Allg. Chem.*, 1994, **620**, 1028.
- 18 R. Korenstein, S. Soled, A. Wold and G. Collin, *Inorg. Chem.*, 1977, **16**, 2344.
- 19 V. Gutmann and K. H. Jack, *Acta Crystallogr.*, 1951, **4**, 244.
- 20 P. Ehrlich, F. Ploeger and G. Pietzka, *Z. Anorg. Allg. Chem.*, 1955, **282**, 19.
- 21 M. Pouchard, M. R. Torki, G. Demazeau and P. Hagenmuller, *C. R. Acad. Sci., Ser. C*, 1971, **273**, 1093.
- 22 J. E. Schirber, B. Morosin, R. W. Alkire, A. C. Larson and P. J. Vergamini, *Phys. Rev. B*, 1984, **29**, 4150.
- 23 M. T. Weller and P. G. Dickens, *J. Solid State Chem.*, 1985, **58**, 164.
- 24 J. B. Parise, E. M. I. McCarron and A. W. Sleight, *Mater. Res. Bull.*, 1987, **22**, 803.
- 25 P. G. Dickens and M. T. Weller, *J. Solid State Chem.*, 1983, **48**, 407.
- 26 J.-L. Fourquet, M.-F. Renou, R. DePape, H. Theveneau, P. P. Man, O. Lucas and J. Pannetier, *Solid State Ionics*, 1983, **9**, 1011.
- 27 J.-L. Fourquet, M.-F. Renou and R. DePape, *Rev. Chim. Miner.*, 1984, **21**, 383.
- 28 P. J. Wiseman and P. G. Dickens, *J. Solid State Chem.*, 1973, **6**, 374.
- 29 P. J. Wiseman and P. G. Dickens, *J. Solid State Chem.*, 1976, **17**, 91.
- 30 R. J. Cava, A. Santoro, D. W. Murphy, S. M. Zahurak and R. S. Roth, *J. Solid State Chem.*, 1983, **50**, 121.
- 31 Inorganic Crystal Structure Database, Release 96/1, FIZ Karlsruhe and Gmelin-Institut, 1996.
- 32 N. N. Zhuravlev, G. S. Zhdanov and R. N. Kuz'min, *Kristallografiya*, 1960, **5**, 553.
- 33 R. N. Kuz'min and G. S. Zhdanov, *Kristallografiya*, 1960, **5**, 869.
- 34 A. Lyons, R. P. Gruska, C. Case, S. N. Subbarao and A. Wold, *Mater. Res. Bull.*, 1978, **13**, 125.
- 35 G. A. Slack and V. G. Tsoukala, *J. Appl. Phys.*, 1994, **76**, 1165.
- 36 C. M. Pleass and R. D. Heyding, *Can. J. Chem.*, 1962, **40**, 590.
- 37 L. D. Dudkin and N. K. Abrikosov, *Zh. Neorg. Khim.*, 1957, **2**, 212.
- 38 V. I. Zobnina and L. D. Dudkin, *Fiz. Tverd. Tela*, 1959, **1**, 1821.
- 39 F. Corà, M. G. Stachiotti, C. R. A. Catlow and C. O. Rodriguez, *J. Phys. Chem. B*, 1997, **101**, 3945.
- 40 J. L. Feldman and D. J. Singh, *Phys. Rev. B*, 1996, **53**, 6273.
- 41 D. J. Singh and I. I. Mazin, *Phys. Rev. B*, 1997, **56**, R1650.
- 42 R. Hoffmann, *J. Chem. Phys.*, 1963, **39**, 1397.
- 43 M.-H. Whangbo and R. Hoffmann, *J. Am. Chem. Soc.*, 1978, **100**, 6093.
- 44 M.-H. Whangbo, R. Hoffmann and R. B. Woodward, *Proc. R. Soc. London, Ser. A*, 1979, **366**, 23.
- 45 R. Hoffmann, *Solids and Surfaces: A Chemist's View of Bonding in Extended Structures*, VCH, Weinheim, 1988.
- 46 T. A. Albright, J. K. Burdett and M. H. Whangbo, *Orbital Interactions in Chemistry*, Wiley, New York, 1985.
- 47 M. Llunell, S. Alvarez, P. Alemany and R. Hoffmann, *Inorg. Chem.*, 1996, **35**, 4683.
- 48 J. H. Ammeter, H. B. Bürgi, J. C. Thibeault and R. Hoffmann, *J. Am. Chem. Soc.*, 1978, **100**, 3686.
- 49 A. Dedieu, T. A. Albright and R. Hoffmann, *J. Am. Chem. Soc.*, 1979, **101**, 3141.
- 50 S. Alvarez, *Table of Parameters for Extended Hückel Calculations*, Universitat de Barcelona, 1993.
- 51 R. Ramirez and M. C. Böhm, *Int. J. Quantum Chem.*, 1986, **30**, 391; 1988, **34**, 571.

Received 14th November 1997; Paper 7/08200B